Image Reconstruction based on Block-based Compressive Sensing

Hanxu YOU, Jie ZHU
Department of Electronic Engineering
Shanghai Jiao Tong University (SJTU)
Shanghai, China

gongzihan@sjtu.edu.cn, zhujie@sjtu.edu.cn

Abstract

The data of interest are assumed to be represented as N-dimensional real vectors, and these vectors are compressible in some linear basis B, implying that the signals can be reconstructed accurately using only a small number of basis function coefficients associated with B. A new approach based on Compressive Sensing (CS) framework which is a theory that one may achieve an exact signal reconstruction from sufficient CS measurements taken from a sparse signal is proposed in this paper. Wavelet-based contourlet transform, block-based random Gaussian image sampling matrix and projection-driven compressive sensing recovery are cooperating together in the new process framework to accomplish image reconstruction. Smoothing is achieved via a Wiener filter incorporated into iterative projected Landweber compressive sensing recovery, yielding fast reconstruction. Different kinds of images are tested in this paper, including normal pictures, infrared images, texture images and synthetic aperture radar (SAR) images. The proposed method reconstructs images with quality that matches or exceeds that produced by those popular ones. Also smoothing was imposed with the goal of improving the quality by eliminating blocking artifacts and quality of reconstruction with smoothing is better to that from pursuits-based algorithm.

Keywords: block-based compressive sensing; contourlet transform; projection driven recovery; smoothing reconstruction.

1. Introduction

The Shannon-Nyquist sampling theorem (Abdul,1977) claims that one must sample at least two times faster than the signal bandwidth while capturing it without losing information. Many signal processing applications require the identification and estimation of a few significant coefficients from a high-dimensional vector. There is an extensive body of literature on image compression, but the central concept is straightforward: we transform the image into an appropriate basis and then code only the important expansion coefficients. The crux is finding a good transform, a problem that has been studied extensively from both a theoretical and practical standpoint. The most notable product of this research is the wavelet transform; switching from sinusoid-based representations to wavelets marked a watershed in image compression and is the essential difference between the classical JPEG (Pennbaker and Mitchell,1993) and modern JPEG-2000 standards (Skodras, Christopoulos and Ebrahimi, 2001). Image compression algorithms convert high-resolution images into a relatively small bit streams (while keeping the essential features intact), in effect turning a large digital data set into a substantially smaller one. Compressive sensing (CS) (Donoho, 2006) is a way to avoid the large digital data set to begin with and that can build the data compression directly into the acquisition.

Compressive sensing (CS), proposed by Donoho (2006), Emmanuel Cand`es (2006) and Micheal Elad(2007) et al, is a new developing novel theory that permits, under certain conditions, signals to be sampled at sub-Nyquist rates via linear projection onto a random basis while still enabling exact reconstruction of the original signal. As applied to 2D images, however, CS faces several challenges including a computationally expensive reconstruction process and huge memory required to store the random sampling operator. Recently, several fast algorithms, as mentioned by Figueiredo, Nowak, Wright (2007), Do, Gan, Nguyen, Tra (2008), Haupt and Nowak (2006), have been developed for CS reconstruction, while the latter challenge was addressed in the works (Gan, 2007) using a block-based sampling operation. Projection-based Landweber iterations were proposed to accomplish fast CS reconstruction while simultaneously imposing smoothing with the goal of improving the reconstructed-image quality by eliminating blocking artifacts.

In this work, we propose this same basic framework of block-based CS sampling to replace the traditional sampling and compressing process. We will address their advantages and merits in detail, and give the comparisons with the classical JPEG and modern JPEG-2000 standards. Different transforms (e.g., wavelet transform, contourlet transform and cosine transform) and different kinds of images (including normal pictures, infrared images, texture images and synthetic aperture radar (SAR) images) are tested in the experiments. Results shows that CS reconstruction which is based on directional transform (contourlet transform) outperforms equivalent reconstruction using common wavelet and cosine transforms.

This work was supported by the National Natural Science Foundation of China (NSFC) under Grants 61271349 and 61371147.

We arrange the paper as follows: the background of Compressive Sensing are depicted in section 2; in section 3 we provide the contourlet transform (Do and Vetterli, 2005) and sampling strategy; the thresholding parameter associated with projection Landweber recovery algorithm is discussed in section 4. And the experiments and comparisons are given subsequently. Finally we summarize our results and prospect our future work.

2. Background of Compressive Sensing

Consider a real-valued, one-dimensional, discrete-time signal x, written as x(n), n=1,2,…,N, and an orthonormal basis, represented in terms of N×1 vectors $\{\psi_i\}_{i=1}^{N}$ with the vectors $\{\psi_i\}$ as its columns, thus $x = \sum_{i=1}^{N} s_i\psi_i$ or $x = \psi s$can be obtained, where s is the N×1 vector of coefficients $s_i = \langle x, \psi_i \rangle = \psi_i^T x$. Supposing K elements of the s_i coefficients are nonzero or largest and (N-K) are zero or negligible, x is called K-sparse or compressible, in which case we are interested. Quite often, the requisite sparsity will exist with respect to some transform Ψ.

According to a common linear measurement course $y_i = \langle x, \phi_j \rangle$, the inner products between x and $\{\phi_j\}_{j=1}^{M}$ can be calculated. Thereafter a compressed signal representation is acquired directly by compressive sensing, which is indeed only M dimensions thus avoiding N samples in data acquisition system. By substituting Ψ and arranging ϕ_j^T as rows in an M×N matrix Φ and consequently $\Theta = \Phi\Psi$ being an M×N sensing matrix, the measurements y can be written as follow:

$$\mathbf{y} = \mathbf{\Phi x} = \mathbf{\Phi\Psi s} = \mathbf{\Theta s} \tag{1}$$

How we recover the signal? In this case, the key to CS recovery is the production of a sparse set of significant transform coefficients $\boldsymbol{s}$.

However, the CS theory tells us that when the matrix $\mathbf{\Theta} = \mathbf{\Phi\Psi}$ has Restricted Isometry Property (RIP) (Baraniuk, Davenport, DeVore and Wakin, 2008),then it is indeed possible to recover the *K* largest coefficients $\boldsymbol{s}$. The RIP is closely related to an incoherency property between $\mathbf{\Psi}$ and $\mathbf{\Phi}$, where the rows of $\mathbf{\Phi}$ do not provide a sparse representation of the columns of $\mathbf{\Psi}$and vice versa. The RIP and incoherency hold for many pairs of bases, including for example, delta spikes and Fourier sinusoids, or sinusoids and wavelets. When RIP holds, the idea recovery procedure searches for the $\boldsymbol{s}$ with the smallest ℓ_0 norm consistent with the observed **y**.

$$\hat{\boldsymbol{s}} = \arg\min\|\boldsymbol{s}'\|_0 \ \text{ such that } \ \mathbf{\Theta s}' = \boldsymbol{y} \tag{2}$$

This optimization will recover a *K*-sparse signal with high probability, but unfortunately solving formula (2) is a non-deterministic polynomial (NP) hard problem, and several alternative solution procedures have been proposed. Perhaps the most prominent of these is basis pursuit (BP) (Chen, Donoho and Saunders,1998) which applies a convex relaxation to the ℓ_0 norm problem resulting in an ℓ_1 norm optimization.

$$\hat{\boldsymbol{s}} = \arg\min\|\boldsymbol{s}'\|_1 \ \text{ such that } \ \mathbf{\Theta s}' = \boldsymbol{y} \tag{3}$$

Although BP can be implemented effectively with linear programming, its computational complexity is often high, leading to recent interest in reduced complexity relaxations as well as in greedy BP variants, including matching pursuits (MP), orthogonal matching pursuits (OMP) and sparsity adaptive matching pursuits (SAMP). Such algorithms significantly reduce computational complexity at the cost of lower reconstruction quality.

As an alternative to the pursuits class of CS reconstruction, techniques based on projections have been proposed already (Haupt and Nowak, 2006). Algorithms of this class form $\hat{\boldsymbol{s}}$ by successively projecting and thresholding; for example, the reconstruction in 0 starts from some initial approximation $\hat{s}^{(0)}$ and forms the approximation at iteration i+1 as follows:

$$\hat{\hat{s}}^{(i)} = \hat{s}^{(i)} + \frac{1}{\gamma}\Psi\Phi^T(y - \Phi\Psi\hat{s}^{(i)}) \tag{4}$$

$$\hat{s}^{(i+1)} = \begin{cases} \hat{\hat{s}}^{(i)}, & \left|\hat{\hat{s}}^{(i)}\right| \geq \mathcal{T}^{(i)} \\ 0, & else \end{cases} \tag{5}$$

Here, γ is a scaling factor uses the largest eigenvalue of $\Phi^T\Phi$), while $\mathcal{T}^{(i)}$ is a threshold set appropriately at each iteration. It is straightforward to see that this procedure is a specific instance of a projected Landweber (PL) algorithm. Like the greedy algorithms of the pursuits class, PL-based CS reconstruction also provides reduced computational complexity. Additionally, and perhaps more importantly, the PL formulation offers the possibility of easily incorporating additional optimization criteria (Mun and Fowler,2009).

3. Contourlet Transform and Sampling Strategy

3.1 Contourlet Transform

Two prominent families of such directional transforms are contourlets and complex-valued DWT. The contourlet transform preserves interesting features of the traditional DWT, namely multiresolution and local characteristics of the signal, and, at the expense of a spatial redundancy, it better represents the directional features of the image. The directional filter bank (DFB) is the key tool to capture the high frequency elements of images whereas grips low frequency elements poorly.

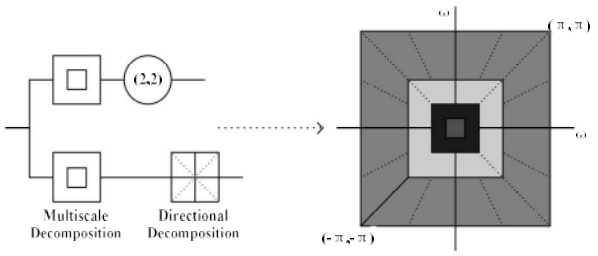

Fig.1. Pyramid Directional Filter Bank (PDFB)

Therefore, a multi-resolution scheme is combined to remove them before the DFB, and thus Laplace pyramid (LP) is considered to allow further sub-band decomposition to be affected on its bandpass images which can be nourished into a DFB to efficiently track down the directional information. We call it pyramidal directional filter bank (PDFB) in respect that

LP is iterated frequently on the coarse image while DFB holding the fine image allowing for a different number of directions at each scale. The illustration is showed in Fig.1. It has the redundancy of 33% owing to the LP, and a perfect reconstruction.

3.2 Sampling strategy

There are numerous matrices working well with compressive sensing framework. It is somewhat surprising that the measurement matrix can be a random, noise-like matrix, for example i.i.d Bernoulli or Gaussian random variables. And in many cases the measurement matrix is a casual, quasi-Toeplitz matrix.

In block-based compressive sensing (BCS), the two dimensional image is divided into $M_B \times M_B$ blocks and sampled with an ordinary random Gaussian matrix in our experiments. That is, suppose that $\boldsymbol{x}_i$ is a vector representing, in raster-scan fashion, block *i* of input data $\boldsymbol{X}$. The corresponding $\boldsymbol{y}_i$ is then

$$\boldsymbol{y}_i = \Phi_B \boldsymbol{x}_i \tag{6}$$

Where Φ_B is an $M_B \times B^2$ orthonormal measurement matrix with $M_B = [\frac{M}{N} B^2]$, $[\cdot]$ is to round down to the nearest integer.

$$\Phi = \begin{bmatrix} \Phi_B & 0 & \cdots & 0 \\ 0 & \Phi_B & & 0 \\ \vdots & & \ddots & \vdots \\ 0 & 0 & \cdots & \Phi_B \end{bmatrix} \tag{7}$$

Using BCS rather than random sampling applied to the entire raw data $\boldsymbol{X}$ has several merits. First, the measurement operator Φ_B is conveniently stored and employed because of its compact size. Second, the encoder does not need to wait until the entire image is measured, but may send each block after its linear projection. Last, an initial approximation $\boldsymbol{X}$ with minimum mean squared error can be feasibly calculated due to the small size of Φ_B . Here we employ blocks of size *B*=32.

4. Theresholding Parameter

As originally described in the work (Haupt and Nowak, 2006) , projection Landweber (PL) algorithm used hard thresholding in the form of (5). To set a proper $\mathcal{T}$ for hard thresholding, we employ the universal threshold method of soft-thresholding. Specifically, in (5),

$$\mathcal{T}^{(i)} = \lambda \sigma^{(i)} \sqrt{2 log K} \tag{8}$$

Where λ is a constant control factor to manage convergence, and *K* is the number of the transform coefficients. As in 0, $\sigma^{(i)}$ is estimated using a robust median estimator,

$$\sigma^{(i)} = \frac{median(|\hat{x}^{(i)}|)}{0.6745} \tag{9}$$

Hard thresholding inherently assumes independence between coefficients. However, bivariate shrinkage is better suited to directional transforms in that it exploits statistical dependency between transform coefficients and their respective parent coefficients, yielding performance superior to that of hard thresholding. A non-Gaussian bivariate distribution was proposed for the current coefficient and its lower-resolution parent coefficient based on an empirical joint histogram of DWT coefficients. However, it is straightforward to apply this process to any transform having a multiple-level decomposition, such as the directional transforms we consider her. Specifically, given a specific transform coefficient ξ and its parent coefficient ξ pin the next coarser scale, the T(·) operator in PL is the MAP estimator of ξ,

$$\mathrm{T}(\xi, \lambda) = \frac{\left(\sqrt{\varepsilon^2 + \varepsilon_p^2} - \lambda \frac{\sqrt{3\sigma^{(i)}}}{\sigma_\xi}\right)_+}{\sqrt{\varepsilon^2 + \varepsilon_p^2}} \cdot \xi \tag{10}$$

Where $(f)_+ = 0 \; for \; f < 0$ else $(f)_+ = f$. $\sigma^{(i)}$ is the median estimator of (9) applied to only the finest-scale transform coefficients; and, again, λ is a convergence-control factor. Here, is the marginal variance of coefficient ξ estimated in a local 3×3 neighborhood surrounding ξ as in the paper (Endur and Selesnick, 2002).

5. Experimental Result

To evaluate the proposed method on image reconstruction, we deploy several experiments within the BCS framework coupled with PL recovery algorithm.

Tests are processed on Core 2 CPU 2.53 GHz 2.53 GHz, 2.00GB memory computer. The test data are including normal pictures, infrared images, texture images (Lazebnik, Schmid and Ponce, 2005) and synthetic aperture radar (SAR) images (Cumming and Wong, 2005). Size of samples is set to 512*512. Samples are showed in Fig.1.

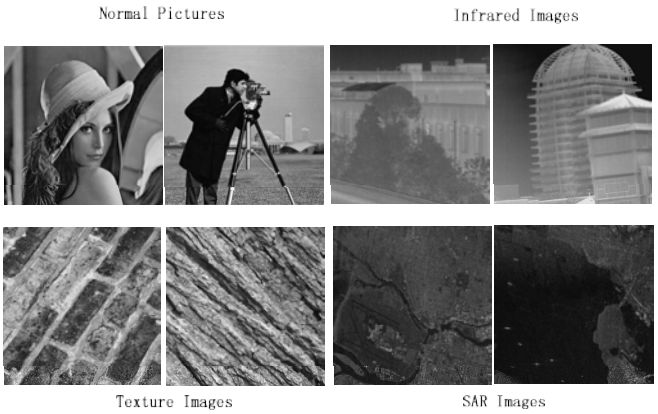

Fig.2. Samples (512*512) used in tests.

5.1 results in different sampling ratio

To test the effectiveness of different sampling ratio, M/N, we choose contourlet domain as the sparse domain in which we sampled Lena (512*512) at several different ratio with random Gaussian matrix. BCS coupled with PL algorithm are applied to acquire the reconstructed image. Fig. 3 shows the experimental visual impression results.

We note that blocking artifacts is eliminated while yielding BCS coupled with projected Landweber recovery. The clearness of reconstruction is along with the sampling ratio, the bigger the ratio, the clearer the reconstruction.

5.2 results in different transform

The transform domain is the important component of BCS framework. Whether data are sparse or not is due to the transform domain. Here we arrange three different sparse domains to test how they affect the quality of reconstructed image. The three transform methods are DCT, DWT and contourlet transform respectively. Table 1-4 compare PSNR for several different transform at several measurement ratios, M/N.

The results indicate that the method proposed in this paper with contourlet transform achieves the best performance while comparing to DCT and DWT at most situation. When processing normal pictures (e.g., Lena, camera man), even the ratio is 0.1, the PSNR is still bigger than 27 dB. The quality of infrared images is best, though the performance of recovering texture images are not as good as others, the PSNR of texture images are still bigger than 22 dB.

Fig.3. Lena images reconstruct by BCS at several different measurement ratios.

	Sampling Ratio (M/N)				
	0.1	0.3	0.5	0.7	0.9
DCT (dB)	26.9312	32.9196	37.6894	42.8479	51.0102
DWT (dB)	26.7073	34.1173	38.1720	42.9766	50.1631
contour-let (dB)	27.0130	33.4483	39.2668	44.2272	51.4630

Table 1: PSNR of normal picture construction

	Sampling Ratio (M/N)				
	0.1	0.3	0.5	0.7	0.9
DCT (dB)	30.5914	39.3815	42.1293	47.5500	54.1839
DWT (dB)	31.8296	39.6365	43.4529	47.2825	53.6248
contour-let (dB)	32.7676	39.4583	43.6540	47.6550	54.3889

Table 2: PSNR of infrared image construction

5.3 compared with other recovery algorithm

There are many compressed sensing (CS) recovery algorithms that have been proposed in recent years. Fig. 4 compares PSNR for Lena constructed by several recovery algorithms, like Compressive Sampling Matching Pursuit (CoSaMP) (Deanna and Tropp, 2001), Orthogonal Matching Pursuit (OMP) (Tropp and Gilbert, 2007), Subspace Pursuit (SP) (Wei and Milenkovic, 2009), Iteratively Reweighted Least Square (IRLS) (Rick and Yin, 2008). Experimental results indicate that the proposed BCS is better than others, though it costs more processing time. PSNR of BCS coupled with PL recovery is about 10 dB bigger that others at every sampling ratios. The fastest recovery algorithm is OMP, and the most comparable algorithm is IRLS.

	Sampling Ratio (M/N)				
	0.1	0.3	0.5	0.7	0.9
DCT (dB)	21.5634	26.5158	30.5417	34.8218	41.9503
DWT (dB)	22.6660	27.5789	31.7323	35.8283	42.0184
contour-let (dB)	22.6698	27.5935	31.6669	36.2512	43.0598

Table 3: PSNR of texture image construction

	Sampling Ratio (M/N)				
	0.1	0.3	0.5	0.7	0.9
DCT (dB)	24.1353	25.7467	27.4719	29.8822	34.7068
DWT (dB)	24.6089	26.3536	28.2731	30.8574	35.8162
contour-let (dB)	24.4337	26.2443	28.0803	30.5767	35.4295

Table 4: PSNR of SAR image construction

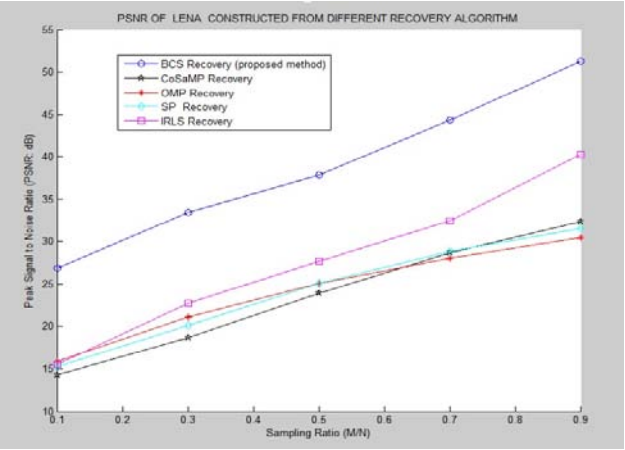

Fig.4. PSNR of Lena reconstructed from different recovery algorithm at several different measurement ratios.

6. Conclusion

Recent theory of Compressive Sensing (CS) provides us with a novel concept that an unknown sparse signal can be exactly recovered with an overwhelming probability even with highly sub-Nyquist-rate samples. These characteristics of CS have attracted many attentions in radar applications. In this paper, we examined the use of recently proposed block-based compressive sensing (BCS) coupled with PL recovery algorithm. Through comparing the quality of different kinds of images, it shows that it works best in infrared images, and when dealing with texture images, the performance of reconstruction is reducing. Other popular CS algorithms are also tested in this paper, results show that the proposed method reconstruction is promoting not only sparsity but also smoothness. The proposed method encourages superior image quality, particularly at infrared images. However, as we can see, lots of work is waiting to be settled because the reconstruction performance has not arrived at its peak yet. As we all know the measurements are not the full information of the resource, sparing samples should always be in accordance with the overall power budget and the waveform design and sampling techniques should consider, hence some kind of reweighing and denoising steps should be introduced to the recovery stage.

7. References

Abdul Jerri. (1977): The Shannon Sampling Theorem—Its Various Extensions and Applications: A Tutorial Review, *Proceedings of the IEEE* **65**: 1565–1595.

W.B. Pennbaker and J.L. Mitchell. (1993): *JPEG Still Image Data Compression Standard*. New York: Springer-Verlag,.

A. Skodras, C. Christopoulos, and T. Ebrahimi. (2001): The JPEG2000 still image compression standard, *IEEE Signal Processing Mag***18**: 36–58.

D. L. Donoho. (2006): Compressed Sensing, *IEEE Trans. on Info. Theory* **52**(4): 1289–1306.

E. Cand`es, J. Romberg and T. Tao. (2006): Robust uncertainty principles: Exact signal reconstruction from highly incomplete frequency information, *IEEE Trans. on Info.Theory* **52**(2): 489–509.

M. Elad. (2007): Optimized Projections for Compressed Sensing, *IEEE Trans. on Signal Process* **55**(12): 5695–5702.

M. A. T. Figueiredo, R. D. Nowak, and S. J. Wright. (2007): Gradient projection for sparse reconstruction: Application to compressed sensing and other inverse problems, *IEEE Journal on Selected Areas in Communications* **1**(4): 586–597.

T. T. Do, L. Gan, N. Nguyen, and T. D. Tra. (2008): Sparsity adaptive matching pursuit algorithm for practical compressedsensing, *in Proceedings of the 42th Asilomar Conference on Signals, Systems, and Computers,* Pacific Grove, California.

J. Haupt and R. Nowak. (2006): Signal reconstruction from noisy random projections, *IEEE Transactions on Information Theory***52**(9): 4036–4048.

L. Gan. (2007): Block compressed sensing of natural images, *in Proceedings of the International Conference on Digital Signal Processing*, Cardiff, UK.

M. N. Do and M. Vetterli. (2005): The contourlet transform: An efficient directional multiresolution image representation, *IEEE Transactions on Image Processing* **14**(12): 2091–2106.

R. Baraniuk, M. Davenport, R. DeVore, M. Wakin. (2008): A simple proof of the restricted isometry property for random matrices. *Constructive Approximation* **28**(3): 253-263.

S. S. Chen, D. L. Donoho, and M. A. Saunders. (1998): Atomicdecomposition by basis pursuit, *SIAM Journal on Scientific Computing*, vol. **20**(1): 33–6.

J. Haupt and R. Nowak. (2006): Signal reconstruction from noisy random projections, *IEEE Transactions on Information Theory* **52**(9): 4036–4048.

S. Mun and J. E. Fowler. (2009): Block compressed sensing of images using directional transforms, *Image Processing (ICIP), 16th IEEE International Conference on*.

D. L. Donoho. (1995): De-noising by soft-thresholding, IEEE Transactions on Information Theory **41**(3): 613–627.

S. Lazebnik, C. Schmid and J. Ponce. (2005): A Sparse Texture Representation Using Local Affine Regions, *IEEE Transactions on Pattern Analysis and Machine Intelligence* **27**(8): 1265-1278.

I. G. Cumming and F. H. Wong. (2005) Digital Processing of Synthetic Aperture Radar Data. Artech House.

L. S. Endur and I. W. Selesnick. (2002): Bivariate shrinkage functions for wavelet-based denoising exploiting interscale dependency, IEEE Transactions on Signal Processing **50**(11): 2744–2756.

N. Deanna and J. A. Tropp. (2001): Cosamp: iterative signal recovery from incomplete and inaccurate samples, *Communications of the ACM* **53**(12): 93-100,.

J. A.Tropp and A. C. Gilbert. (2007): Signal recovery from random measurements via orthogonal matching pursuit, *IEEE Transactions on Information Theory* **53**(12): 4655-4666, 2007.

D. Wei, and O. Milenkovic. (2009): Subspace pursuit for compressive sensing signal reconstruction, *IEEE Transactions on Information Theory* **55**(5): 2230-2249.

C. Rick and W. Yin. (2008): Iteratively reweighted algorithms for compressive sensing, *IEEE International Conference on Acoustics, Speech and Signal Processing (ICASSP)*.